

# Comparisons Among p-Channel, n-Channel and Mixed n/p -Channel OTFTs

Cristian Ravariu\*, Georgeta Alecu†

\*Politehnica University of Bucharest, The Faculty of Electronics, Telecommunications and Information Technology, Bucharest, Romania, cristian.ravariu@upb.ro

†National Institute for Research and Development in Electrical Engineering ICPE-CA, Bucharest, Romania, georgeta.alecu@icpe-ca.ro

**Abstract** - Some theoretical approaches of an alternative organic semiconductor device are presented in this work. The Organic transistors are based either on n-type or p-type or mixed p/n overlapped layers. The carrier modulation insides different films is carried out by two gates electrodes, as is usual in the thin film transistor field. This paper introduces some novel aspects for these kinds of organic transistors, selecting a suitable biasing regime. The simulations emphasize a stronger influence on the static characteristics when the superior gate is acted. One of the novelties of this paper concerns the electrical conduction occurrence by two simultaneous channels, in comparison with one volume channel conduction, for different gate voltage regimes. A similar work regime is also encountered in the SOI devices with ultra-thin films that develop a volume channel. The volume channel regime is advantageously when the technology of fabrication of the organic semiconductors on different insulators provides an extremely charged interface, which can degrade the surface currents. Comparisons and applications for both situations - with one volume channel or two accumulation channels - are finally discussed. The vertical n/p junction arose between the upper n-channel and the bottom p-channel, offers novel physical properties and prevented any interaction among channels. The device simulations revealed multiple behaviors, depending on the Top and Bottom Gate voltages, if a positive drain-source voltage is applied.

**Keywords:** organics transistors, thin films, simulations, alternative materials in electronics.

## I. INTRODUCTION

The organic technology provides facile methods of the thin film transistors manufacturing, at room temperature processes as inkjet printing, sol-gel process, roll-to-roll printing, which provides low cost technologies, against the classical lithography from the silicon technology, [1-3].

Even with the last years rapid progress in the organic materials manufacturing [4], an Organic Thin Film Transistor (OTFT) with better characteristics than a Metal Oxide Semiconductor Field Effect Transistor (MOSFET), rests a major issue, [5].

For example, the Organic METal Semiconductor Field Effect Transistor (OMESFET) developed by another researcher group [6], operates at lower voltages than usual OTFT, with better ON/OFF current ratio, but only use the conduction thru a channel with p-type conduction, [6].

The well-known technologies of the Pentacene OTFT transistors frequently demand conduction thru a p-type organic layer, except for a few low band-gap organic polymers. Recently, other authors claim that n-type conduction can be used in conjunction with convenient organic gate dielectrics [7], even in special low band-gap organic semiconductors, where the electrons mobility increases to  $0.05\text{cm}^2/\text{Vs}$ , [8].

Till nowadays, the more performant Organic-TFTs are fabricated by the p-type organic polymers, offering conduction regime with accumulation channel. An additional reason for the n-type organic-TFT avoiding is the electrons entrapping at the semiconductor-oxide interface by hydroxyl groups, present as silanols in the usual  $\text{SiO}_2$  insulator, [8]. OTFTs with pentacene onto a dielectric polymer layer enriched the drain current excursion from 8nA to 80nA at the same gate voltage biasing, [9].

Therefore, in this paper, a mixed solution - with a p-organic layer on an n-organic layer - is considered to enrich the current way. The source to drain conduction is possible by accumulation channels [10] or by volume channels, [5]. In this paper we take into account the possibility to ensure a superior conduction by the superposition of both these two mechanisms. The polyimide material is considered as buried organic insulator and the oxide material is considered as the upper insulator, for the proposed Organic-TFT. The compatibility between the circuit integration technology and the surface oxide is wellknown, while the matching with polyimide material was proved elsewhere, [11]. The expected results envisage a larger current capability by a suitable work regime and alternative functions for these transistors.

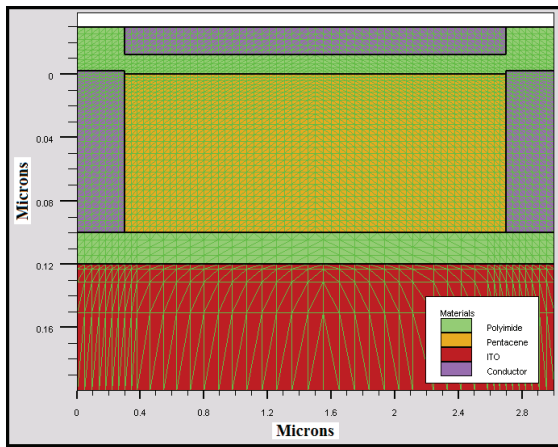
## II. THE DEVICES STRUCTURE AND PHYSICAL PARAMETERS

This organic thin film transistor also belongs to the Semiconductor on insulator SOI transistor class [12], due to similar configuration with sub-100nm organic films placed onto an insulator support from polyimide. Therefore, the back and front gates from SOI architectures [13] are labeled here as bottom and top gates, to be in agreement with the TFT terminology, [6, 7].

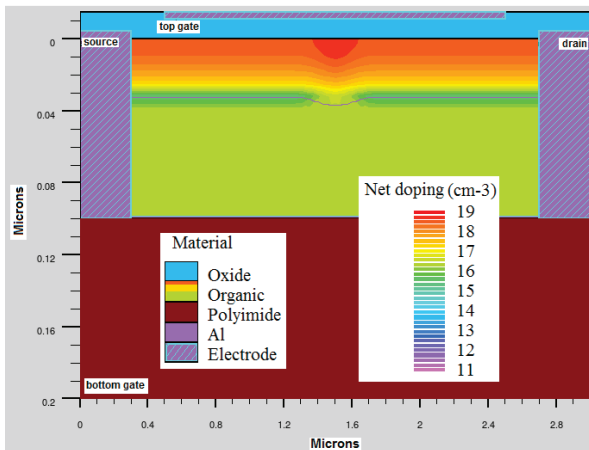
The investigation software tools from this paper involve the Atlas 2D from Silvaco, adapted for our OTFT device. In fig. 1.a is presented the proposed structure besides to the mesh for a sole p-channel transistor or similar

for n-channel and in fig. 1.b is presented the adopted structure with mixed n/p channels with modified geometry. In this last case, the structure gathers an accumulation current localized at the upper interface with oxide and with the inferior interface with polyimide. In this way, multiple conduction routes occur: by upper n-channel and bottom p-channel. However, the metallic shortcut on the vertical direction, achieved by the deep source and drain contacts, ensure a zero current within the pn junction on the Oy axis.

From the material point of view, the organic semiconductor can be depicted either as the default pentacene from the Atlas library [14], or as optimized organic semiconductors from literature [15] simply labeled as Organic.



(a)



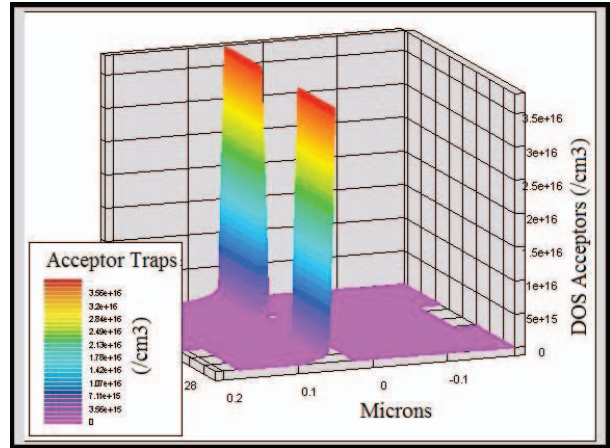
(b)

Fig 1. Materials and doping profile within the O-TFT with (a) sole p-channel; (b) mixed p/n-channels.

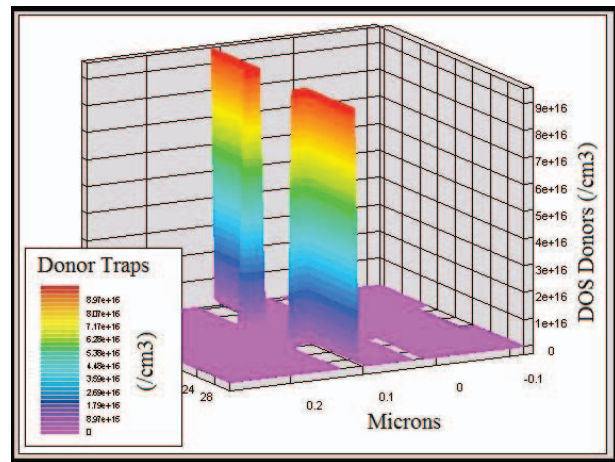
In the literature, the carrier motilities inside the organic semiconductors are typically of  $0.1...1\text{cm}^2/\text{Vs}$ , or more, [16]. We considered an average value of  $0.8\text{cm}^2/\text{Vs}$  in these simulations. In order to make possible both electrons and holes charge transport, the Lowest Unoccupied Molecular Orbital (LUMO), besides to the Highest Occu-

ried Molecular Orbitals (HOMO) - energy levels must be localized as close as possible and the gate dielectrics must suppress the electron capture at the organic-dielectric interface.

In order to be closer to a real behavior, in this paper, the the Density Of States (DOS) are distinctly defined at the organic semiconductor / polyimide interface by for ionized acceptor states -  $g_A=3.75 \times 10^{16}\text{cm}^{-2}$ , fig 2.a, and ionized donor states  $g_D=9.5 \times 10^{16}\text{cm}^{-2}$ , fig. 2.b, [17].



(a)



(b)

Fig. 2. The ionized states density taken into account in simulations: (a) for acceptors; (b) for donors.

For the presented OTFT structure, the aluminum contacts provide a Schottky barrier, while the gold contacts offers better ohmic contacts and they are finally included in simulations. Also the simulations show a strong dependence of the contact resistance on the doping concentrations in the n or p type layers. On the other hand, the contact resistances are variable for different gates biasing, due to the carriers concentration ranging, [15].

The physical parameters of the standard pentacene, noted as Pentacene [14], enhanced new organic semiconductors noted as Organic [15, 19] and polyimide as insu-

lators [20] are included in the Atlas models by the "material" instruction and centralized in table 1. Those parameters that are missing from table 1, for pentacene, organic or insulators, get the default values from the Atlas library, [14]. The sizes and doping concentrations of each layer are selected from a real organic technology [11-21], and they are indicated as main references in table 1. The n-type layer is defined by a Gaussian doping concentration, with a maximum value of  $10^{19} \text{ cm}^{-3}$ , while the p-type substrate has  $10^{17} \text{ cm}^{-3}$ .

TABLE I.  
INITIAL DEVICE CHARACTERISTICS

Material	Thickness ( $\mu\text{m}$ )	$E_G$ (eV)	Mobility ( $\text{cm}^2/\text{Vs}$ )
n-Pentacene	40 <sup>[15]</sup>	2.11 <sup>[21]</sup>	$1 \times 10^{-5}$ , <sup>[21]</sup>
p-Pentacene	60 <sup>[9]</sup>	2.11 <sup>[21]</sup>	$4 \times 10^{-4}$ , <sup>[21]</sup>
n-Organic	40 <sup>[15]</sup>	1.20 <sup>[19]</sup>	0.80 <sup>[15]</sup>
p-Organic	60 <sup>[9]</sup>	1.21 <sup>[19]</sup>	0.80 <sup>[15]</sup>

### III. FIRST ATLAS SIMULATIONS

The Atlas input file is prepared to simulate electrical conduction thru organic materials, activating some key parameters in the "model" instruction: pfmob singlet langevin, to activate the Poole-Frenkel mobility model and the Langevin recombination for the existent carriers, [14].

In Atlas 2D output files, the drain currents are expressed in Amperes per  $1 \mu\text{m}$ , as default depth. Therefore, in our simulations, the current densities are more relevant than the currents itself.

The potential distribution over the mixed OTFT structure is presented in fig. 3, accordingly with an expecting work regime, for low positive drain voltage and negative top-gate voltage and also negative bottom-gate voltage. In another work regime, the drain voltage is increased, when the mixed device is biased at  $V_S=0\text{V}$ ,  $V_D=40\text{V}$ ,  $V_{TG}=-10\text{V}$  and  $V_{BG}=30\text{V}$ , the maximum electric field occurs on a  $0.2 \mu\text{m}$  length of oxide, between the edges of top gate and drain electrodes.

Subsequently, the maximum electric field reaches  $2.5 \times 10^6 \text{ V/cm}$ , still lower than  $1.1 \times 10^7 \text{ V/cm}$ , but under increasing alert for the critical electric field in the right corner of the oxide, near the drain contact. Hence, a limit drain voltage can be  $+40\text{V} \dots +50\text{V}$  to avoid the breakdown. A thicker polyimide provides a lower residual current thru polyimide versus oxide, at the same voltages. For the device safety, the gate currents are monitored. After simulations, the top and bottom gate current densities possess few orders of magnitudes lower than the drain current, so far away from the breakdown conditions and far away from the loss of the gate control.

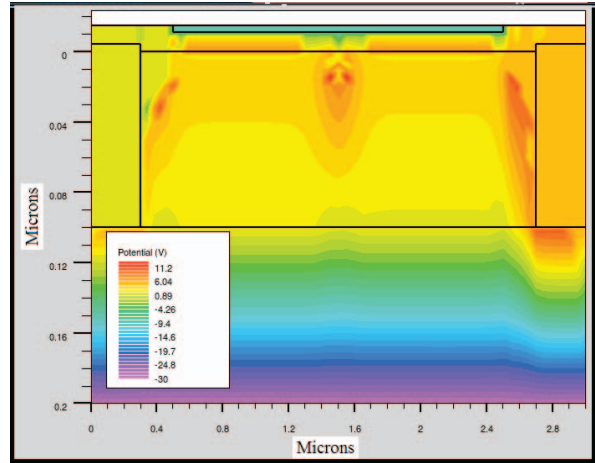
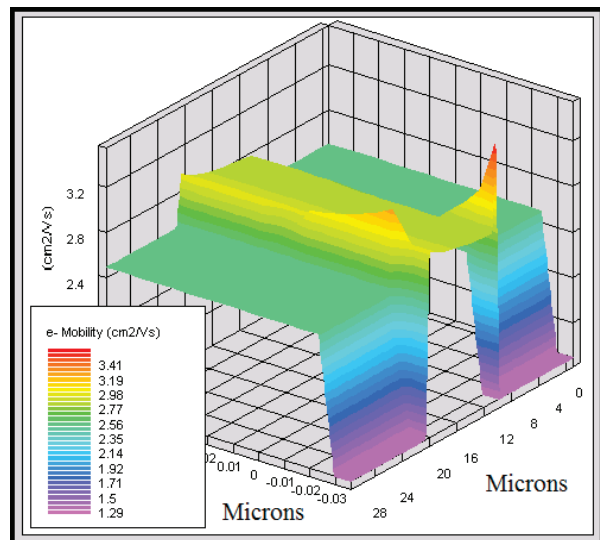


Fig 3. The potential distribution at  $V_S=0\text{V}$ ,  $V_D=+4\text{V}$ ,  $V_{TG}=-10\text{V}$  and  $V_{BG}=-30\text{V}$  in mixed OTFT.

Because the mixed OTFT structure comprises a vertical n/p junction, two types of electrical carriers ensure the longitudinal conduction, as in any pn junction.

A top gate biased at negative voltage can foster the holes accumulation. An additional negative bottom gate voltage enhances the holes accumulation, while positive bottom gate voltage depletes the p-type film, fig. 3. Holes accumulation occurs near the polyimide interface for  $V_{BG}=-30\text{V}$ , up to  $2 \times 10^{18} \text{ cm}^{-3}$ , higher than the native doping concentration of  $10^{17} \text{ cm}^{-3}$ , while holes accumulation occurs near the oxide interface for  $V_{TG}=-10\text{V}$ , up to  $9 \times 10^{19} \text{ cm}^{-3}$ . In this case, an electrons volume channel coexists with the upper holes surface channel, near the source vicinity. The work regime with positive top gate voltage provides two conduction channels, near oxide and polyimide interfaces, depending on the bottom gate biasing.

Figure 4 presents a comparison between the electrons and holes mobility, under usual biasing conditions.





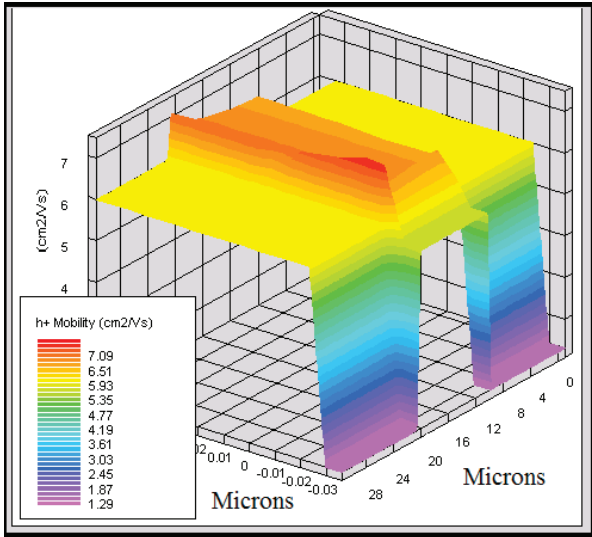


Fig 4. The electrons and holes concentration for different top and bottom gate voltages.

The specific models included in Atlas to capture the organic semiconductors becomes obviously, due to the results with higher holes mobilities and lower electron mobilities (opposite to the inorganic semiconductors), as is specifically encountered in literature, [22].

#### IV. STATISTIC REGIME ANALYSIS

The output characteristics simulations,  $I_D$ - $V_{DS}$ , consists in drain-source voltage ranging from 0V to positive values at maximum +40V, keeping a negative bottom gate voltage and associating different top-gate voltages, fig. 5. In the simulations from fig. 5, the organic semiconductor noted by organic, is envisaged. The current decreases when the negative top or bottom voltages increase in modulus, due to the n-channel diminishing.

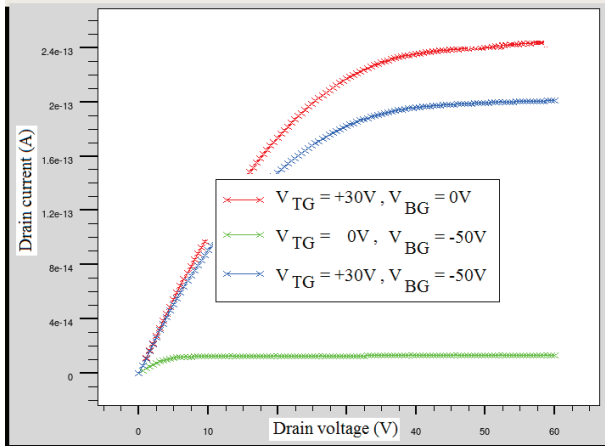


Fig 5. The output characteristics at different top and bottom gate voltages.

Selecting the optimum "organic" semiconductor, the drain current reaches in the saturation region for a saturation voltage,  $V_{DSat}$  of minimum +5V and maximum +42V in fig. 5. The maximum drain current reaches a value of  $2.38 \times 10^{-13}$  A that is 2.3 times higher than in a previous

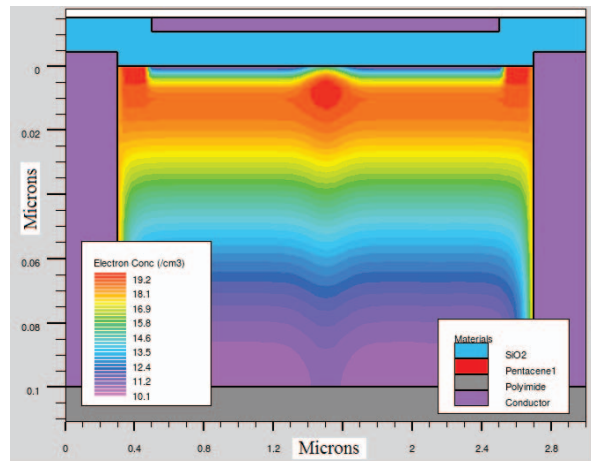
analysis [11], when  $I_D$  was 100fA. Now, the maximum saturated drain current of 238fA occurs for  $V_{TG}=+30$ V,  $V_{BG}=0$ V, instead old conditions for  $V_{TG}=+10$ V,  $V_{BG}=+50$ V.

In this study results that a higher positive top gate voltage produces higher drain currents. A lower dependence of the drain current on the bottom gate voltage is simulated.

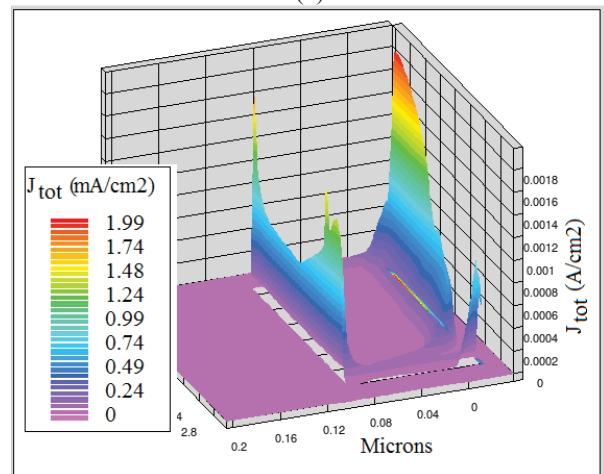
#### V. DISCUSSIONS

The applications of the proposed OTFT are in agreement with the applied voltages in each work regime. Because the n and p layers possess different doping concentrations, the conduction through the longitudinal n-channel is stronger than the conduction through the longitudinal p-channel.

The conduction superiority has to be established by the static characteristics analysis, forcing the device to use a p-type channel or a n-type channel. This evolution is emphasized once for a maximum electron concentration reached deeply in the n-type film of  $10^{19}$  cm<sup>-3</sup>, but rather closer to the oxide layer, fig. 6.a.



(a)



(b)

Fig 6. The electron concentration through the proposed OTFT with overlapped channels as contours traces proving a thin volume channel onset; two accumulation channels onset at  $V_S=0$ V,  $V_D=40$ V,  $V_{TG}=10$ V.

When positive voltages are applied on both gate terminals, two accumulation channels occur near the interfaces with oxide and with polyimide, fig. 6.b. This work regime with two simultaneous channels acted by two gates represents the main explanation to support a 2.3 higher drain current during the saturation regime.

If the positive voltage is applied on the top-gate, ( $V_{TG}>0$ ), the electron concentration increases in a thin volume channel, at 10nm close under the upper oxide interface (where  $n > 10^{19} \text{cm}^{-3}$ ), offering the specific volume channel conduction way [4], with a maximum of efficiency now, 2.3 times higher drain current. Whether the work regime is changed ( $V_{TG}<0$  or  $V_{BG}>0$ ), the holes channel is onset within the p-type layer and systematically the hole current density rests much lower than the electron current density, due to the initial asymmetry in the doping concentrations. To capture an as favorable as possible work regime for the holes transport, it is necessary to invert the biasing (e.g. for  $V_{TG}>0$ ,  $V_{BG}<0$ ), to increase the hole concentration  $p > 10^{19} \text{cm}^{-3}$  near the polyimide interface, so that two distinct accumulation channels occurs and both get the same order of magnitude for the current density,  $j_{p, n} = 1.2 \dots 1.8 \text{ mA/cm}^2$ , fig. 6.b. The localization of these two channels is near the oxide interface and near the polyimide interface. In this case, the vertical n/p junction is reverse biased, with two depleted regions, n-type and p-type that touch each other by the median coordinate of the organic mixed layers. This reverse bias prevents any leakage between the upper n-channel and the bottom p-channel, ensuring a firm behavior of the device.

Some comparisons of the main voltages and saturated drain current for the proposed device biased at  $V_{TG}>0$ , with similar organic thin film transistors, are presented in table 2.

TABLE II.  
THE OTFTS DEVICE PARAMETERS

Parameters	$ V_G $ (V)	$ I_{d, \max} $ ( $\mu\text{A}$ )	$V_{Dsat}$ (V)
Actual OTFT	1 ... 30	0.238	2...42
Other OTFT	17... 33 <sup>[22]</sup>	0.102 <sup>[11]</sup>	24...54 <sup>[21-29]</sup>

The studied organic OTFTs are suitable for the industrial low power display, due to a low drain current consumption, versus other variants, [22]. Also the organic devices are suitable for any biomimetic applications, which require carriers mobility under  $0.1 \text{ cm}^2/\text{Vs}$ , [24] and transducer with organic materials as biocompatible interfaces, [25-29].

The volume channel regime is advantageously when the technology of fabrication of the organic semiconductors on different insulators provides an extremely charged interface, which can degrade the surface currents.

## VI. CONCLUSIONS

This paper studied some new configurations of Organic Thin Film Transistors, which usually used a sole p-channel, or a sole n-channel. When a mixed structure with n-type layer on a p-type layer was used in the organic semiconductor region, some novel kinds of conduction channels occurred. The vertical n/p junction arose between the upper n-channel and the bottom p-channel, offers novel physical properties and prevented any interaction among channels.

The device simulations revealed multiple behaviors, depending on the Top and Bottom Gate voltages, if a positive drain-source voltage is applied.

## ACKNOWLEDGMENT

This work was partially supported by POSDRU/89/1.5/S/62557 Project.

*Received on October 6, 2016.*

*Editorial Approval on November 20, 2016.*

## REFERENCES

- [1] Alejandro de la Fuente Vornbrock, Donovan Sung, Hongki Kang, Rungrot Kitsomboonloha, Vivek Subramanian, Fully gravure and ink-jet printed high speed pBTTT organic thin film transistors, Organic Electronics, Volume 11, Issue 12, pp. 2037-2044, 2010.
- [2] K. Bock, Polymer electronics systems—Polytronics, Proceedings of IEEE, vol. 93, no. 8, pp. 1400–1406, 2005.
- [3] Tariel Ebralidze, Nadia Ebralidze, Giorgi Mumladze, Molecular Aggregations and Anisotropy Photoinduction in Organic Compounds, Optics. Vol. 3, No. 4, 2014, pp. 33-36.
- [4] C. Ravariu, D. Dragomirescu, F. Babarada, D. Prelipceanu, B. Patrichi, C. Gorciu, D. Manuc, A. Salageanu, Organic Field Effect Transistor OFET Optimization Considering Volume Channel Conduction Mechanism, 38-th IEEE International Annual Conference of Semiconductors, 12-14 Oct, 2015, Sinaia, Romania, pp. 113-117.
- [5] Anita Risteska, Kah-Yoong Chan, Thomas D. Anthopoulos, Aad Gordijn, Helmut Stiebig, Masakazu Nakamura, Dietmar Knipp, Designing organic and inorganic ambipolar thin-film transistors and inverters: Theory and experiment, Organic Electronics, Volume 13, Issue 12, pp. 2816–2824, 2012
- [6] Arash Takshi, Alexandros Dimopoulos, and John D. Madden, Simulation of a Low-Voltage Organic Transistor Compatible With Printing Methods, IEEE Transactions on electron devices, vol. 55, no. 1, pp. 276-282, 2008.
- [7] Satria Zulkarnaen Bisri, Taishi Takenobu, Yohei Yomogida, Hidekazu Shimotani, Takeshi Yamao, Shu Hotta, and Yoshihiro Iwasa, High Mobility and Luminescent Efficiency in Organic Single-Crystal Light-Emitting Transistors, Adv. Funct. Mater., vol. 19, pp. 1728–1735, 2009.
- [8] L.-L. Chua, J. Zaumseil, J.-F. Chang, E.-C. W. Ou, P. K.-H. Ho, H. Sirringhaus, and R. H. Friend, General observation of n-type field effect behavior in organic semiconductors, Nature, vol. 434, no. 7030, pp. 194–199, 2005.
- [9] J. Jakobovic, J. Kovac, M. Weis, D. Hasko, R. Smanek, P. Valent, R. Resel, Preparation and properties of thin parylene layers as the gate dielectrics for organic field effect transistors, Microelectronics Journal, vol. 40, pp. 595– 597, 2009.
- [10] C. Ravariu, Deeper Insights of the Conduction Mechanisms in a Vacuum SOI Nanotransistor, IEEE Transactions on Electron Devices, vol. 63, no. 8, 2016, pp. 3278 - 3283.
- [11] C. Ravariu, D. Dragomirescu, Different Work Regimes of an Organic Thin Film Transistor OTFT and Possible Applications in Bioelectronics, American Journal of Bioscience and Bioengineering, vol. 3, issue 3-1, June 2015, pp. 7-13.

- [12] C. Ravariu, F. Babarada, Modeling and simulation of special shaped SOI materials for the nanodevices implementation, *Hindawi Journal of Nanomaterials*, ID 792759, pp. 1-11, July 2011.
- [13] C. Ravariu, F. Ravariu, A test two-terminals biodevice with lipophylic and hidrophylic hormone solutions, *Journal of Optoelectronics and Advanced Materials JOAM*, vol. 9, nr. 8, pp. 2589-2592, Aug. 2007.
- [14] \*\*\*, Atlas Manual 2012, available at: [www.silvaco.com](http://www.silvaco.com).
- [15] Franziska D. Fleischli, Katrin Sidler, Michel Schaer, Veronica Savu, Jürgen Brugger, Libero Zuppiroli, The effects of channel length and film microstructure on the performance of pentacene transistors, *Organic Electronics*, vol. 12, pp. 336-340, 2011.
- [16] P. Singh, A. Sellinger, A. Dodabalapur, Electron transport in copper phthalocyanines *J. Appl. Phys.*, 107, 044509, 2010.
- [17] G. Bersuker, P. Zeitzoff, G. Brown, and H. R. Huff, Dielectrics for future transistors, *Materials Today*, vol. 7, no. 1, pp. 26-33, 2004.
- [18] Burgi, L.; Richards, T. J.; Friend, R. H.; Sirringhaus, H., Close look at charge carrier injection in polymer field-effect transistors, *J. Appl. Phys.*, vol. 94, issue 9, 6129: 1-9, 2003.
- [19] Prashant Sonar, Samarendra P. Singh, Yuning Li, Mui Siang Soh, and Ananth Dodabalapur, A Low-Bandgap Diketopyrrolopyrrole-Benzothiadiazole-Based Copolymer for High-Mobility Ambipolar Organic Thin-Film Transistors, *Adv. Mater.*, vol. 22, pp. 5409-5413, 2010.
- [20] Stefan Chisca, Ion Sava, Valentina-Elena Musteata, Maria Bruma, Dielectric and conduction properties of polyimide films, *IEEE International Semiconductor Conference CAS 2011*, Volume: 2, pp. 253 - 256, 2011.
- [21] Jana Zaumseil and Henning Sirringhaus, Electron and Ambipolar Transport in Organic Field-Effect Transistors, *Chem. Rev.*, 107, pp. 1296-1323, 2007.
- [22] Hagen Klauk, Organic thin-film transistors, *Chem. Soc. Rev.*, vol. 39, pp. 2643-2666, 2010.
- [23] P. F. Babarada, C. Ravariu, J. Arhip, Electrophysiological Data Processing Using a Dynamic Range Compressor Coupled to a Ten Bits A/D Conversion Port, in *Proceedings IEEE-CCP*, Lisa O'Conner Editor, Conference Publishing Services CPS, IEEE Computer Society, pp. 257-262, 2011.
- [24] G. S. Costa, A. M. Salgado, P. R. G. Barrocas, Advances on Using a Bioluminescent Microbial Biosensor to Detect Bioavailable Hg (II) In Real Samples, *American Journal of Bioscience and Bioengineering*. Vol. 1, No. 3, 2013, pp. 44-48.
- [25] Tae-Jun Ha, Prashant Sonar, Samarendra P. Singh, and Ananth Dodabalapur, Characteristics of High-Performance Ambipolar Organic Field-Effect Transistors Based on a Diketopyrrolopyrrole-Benzothiadiazole Copolymer, *IEEE Transactions on electron devices*, vol. 59, no. 5, pp. 1494-1500, 2012.
- [26] Bremner, Y. Liu, M. Samie, G. Dragffy, A. G. Pipe, G. Tempesti, J. Timmis and A. M. Tyrrell, SABRE: a bio-inspired fault-tolerant electronic architecture, *Bioinspir. Biomim.* IOP, 8 016003, 2013.
- [27] Poornima Mittal, B. Kumar, Y.S. Negi, B.K. Kaushik, R.K. Singh, Channel length variation effect on performance parameters of organic field effect transistors, *Microelectronics Journal*, Volume 43, Issue 12, pp. 985-994, 2012.
- [28] Yoshinori Ishikawa, Yasuo Wada, and Toru Toyabe, Origin of characteristics differences between top and bottom contact organic thin film transistors, *Journal of applied physics*, 107, 053709, 2010.
- [29] Na Liu, Yulei Hu, Jianhua Zhang, Jin Cao, Yinchun Liu, Jun Wang, A label-free, organic transistor-based biosensor by introducing electric bias during DNA immobilization, *Organic Electronics*, vol. 13, pp. 2781-2785, 2012.